# Mathematical reconstruction of color-matching functions

**Javier Romero, Luis Jiménez del Barco, and Enrique Hita**

*Departamento de Fisica Aplicada, Facultad de Ciencias, Universidad de Granada, 18071 Granada, Spain*

Received April 5, 1990; revised manuscript received August 6, 1991; accepted August 16, 1991

We calculate the fast Fourier transforms of the color-matching functions for the CIE 1931 standard observer with reference to the $XYZ$ primaries. From an analysis of the Fourier-transform moduli thus obtained, we were then able to study the sampling theorem to get mathematical formulas that lead to the reconstruction of the color-matching functions at limiting frequencies of 0.02 and 0.05 cycle/nm. This reconstruction proves to be highly reliable at a sampling interval of 10 nm and perfectly acceptable at 25 nm and even wider intervals.

## INTRODUCTION

Some researchers in colorimetry[1–3] have used the Fourier analysis to represent, for example, spectral reflectance functions in terms of frequency-limited functions, that is, those functions whose Fourier transform is 0 above a certain frequency (limiting frequency). Buchsbaum and Gottschalk[2] included a graphic representation of the modulus of the discrete Fourier transform of the color-matching functions for the CIE 1931 standard observer. It can be deduced from these representations that each of the Fourier transforms of the three color-matching functions vanishes above a certain frequency. Barlow[4] reported similar results after applying the Fourier transform to the Smith–Pokorny fundamental spectral sensitivities as did Benzschawel *et al.*[5] by analyzing color-vision mechanisms based on various different models.

In the research of Buchsbaum and Gottschalk[2] it is shown that the modulus of the Fourier transform obtained for the $\bar{y}_\lambda$ function seems to become 0 at a frequency even lower than 0.01 cycle/nm. This result appears to us to be of great interest if our intention is to apply the sampling theorem[6] to the color-matching functions of the standard observer.

In fact, if a function $M(\lambda)$ had a limiting frequency of 0.01 cycle/nm, this would mean that we could sample it at a minimum frequency of 0.02 cycle/nm, i.e., at wavelength intervals of 50 nm, and reproduce it, without losing any information, in the form

$$M(\lambda) = \sum_{n=-\infty}^{+\infty} M\left(\frac{n}{2f_1}\right)\mathrm{sinc}\left[2f_1\left(\lambda - \frac{n}{2f_1}\right)\right], \qquad (1)$$

where $f_1$ is the limiting frequency.

If we consider that $M(\lambda)$ is one of the color-matching functions and take the visible spectrum to be 360–760 nm, where the function has values significantly different from 0, it will be sufficient to sample eight values of the function in order to obtain its analytical representation. This could imply a reduction in the number of experimental measurements needed to determine color-matching functions and also to arrive at analytical expressions for them, which we do not have at present.

In this way our intention has been to achieve a spectral analysis of the color-matching functions for the CIE 1931 standard observer and to study whether the color-matching functions can really be considered as being frequency-limited functions. If this were so, it would be possible to arrive at their theoretical reconstruction with the use of a mathematical expression such as formula (1). Although this equation employs sinc functions, which admittedly are difficult to use experimentally as they decay slowly, mathematically it does permit the reconstruction of color-matching functions with well-known functions, which is our prime intention. From the results of this analysis, we hope to formulate a more efficient experimental methodology and also to obtain mathematical expressions for calculating the color-matching functions. Furthermore, in the research of Barlow[4] and Benzschawel *et al.*[5] some features of the color vision system as a low-pass filter could be deduced. This leads us to be interested in the study of the behavior of color vision mechanisms in the frequency domain.

The problem of reconstructing color-matching functions by this method may be related to the interpolation methods of color-matching function values of Stearns[7] and Erb and Krystek.[8] Actually, these papers were concerned with the analysis of abridgment and truncation problems in the calculation of tristimulus values. While they do indeed elaborate on a prediction method for color-matching functions outside the interval in which the reflectance of an object is measured, this prediction is subject to the calculation method for tristimulus values. However, we will take as our starting point the complete definition of color-matching functions (360–830 nm, $\Delta\lambda = 1$ nm), taking the most significant interval as being between 360 and 759 nm.

As far as the research of Stiles *et al.*[1] is concerned, these authors have designed a model for the representation of spectral reflectances of color objects by the sum of sinc functions. In fact, they generated a family of this type of sum in an attempt to represent the real reflectances with the aim of solving the problem of counting metameric objects. The limiting frequency of their sinc functions is between 0.01 and 0.05 cycle/nm, but they indicate that it is necessary to extend the sum of this type of function to include sinc functions centered outside the visible spectrum in both directions to make an adequate calculation of the tristimulus values associated with the reflectances. In our case we consider that the problem is

0740-3232/92/010025-05$05.00 

somewhat different because, as is shown in formula (1), although we are using sinc functions that decay slowly, they are multiplied by the value of the color-matching function in each wavelength in which they are centered, which means that they can be used only within the visible spectrum.

## FOURIER ANALYSIS OF COLOR-MATCHING FUNCTIONS

First we obtained the fast Fourier transform (FFT's) of the $\bar{x}_\lambda$, $\bar{y}_\lambda$, and $\bar{z}_\lambda$ color-matching functions for the CIE 1931 standard observer between 360 and 759 nm at intervals of $\Delta\lambda = 1$ nm (Ref. 9, pp. 725–734).

Strictly speaking, when carrying out a discrete Fourier transform, one should be certain that the frequency of the sample of the signal (in our case 1 cycle/nm) is equal to or greater than double the limiting frequency; that is, in order to make the transform, we must presume that it will vanish at frequencies of less than 0.5 cycle/nm. Thus, as we have the color-matching functions only as a discrete set of values, we must take it that this is in fact what happens. Previous results of Buchsbaum and Gottschalk[2] and the graphic expressions of the color-matching functions by Wyszecki and Stiles[9] support this idea and lead us to believe that there will be *no contribution at high frequencies*.

However, we know that a function that exists only in a finite interval cannot mathematically be band limited, and therefore, strictly speaking, the sampling theorem does not hold. We may therefore find that the color-matching functions are only approximately band limited and that the application of formula (1) extended only to the visible spectrum will give an analytical representation of the functions that is an approximation to the complete analytical representation.

In order to apply the sampling theorem, we have to presume that the FFT's of the color-matching functions nearly vanish at a determined frequency and that this frequency is the limiting frequency used to apply formula (1). We would then have to compare graphically and numerically the reconstruction values with the real values of the corresponding function. Furthermore, the limiting frequency that we are considering would also be affected by the application of the sampling theorem from a Fourier transform that is discrete and not continuous, which is when such a frequency has its exact significance.

To obtain a fine sampling of the FFT modulus and based on the fact that color-matching functions take 0 values in the ultraviolet and the infrared regions, we added 1800 0's equally spaced at 1-nm intervals to each end of the visible spectrum considered and then used 4000 samples to make each of the FFT's ($\Delta f = 0.00025$ cycle/nm). This $\Delta f$ is 12.5 times better than the resolution in Buchsbaum and Gottschalk, which is $\Delta f = 0.003125$ cycle/nm.

The FFT moduli for these three functions appear in Fig. 1. The value for $f = 0$ cycle/nm, 0.0534, is the result of the sum of all the values of each function divided by half the number of samples. As the sum of the three color-matching functions is the same, this value is the same for the three curves of Fig. 1.

We may presume that the FFT's for the three functions nearly vanish, although at a different limiting frequency for each. This result is to be expected because $\bar{y}_\lambda$ and $\bar{z}_\lambda$, for example, are similar in form, although the latter is narrower, which makes its transform vary more slowly with the frequency.

In this way the modulus value for the Fourier transform of the $\bar{y}_\lambda$ function for a frequency of 0.02 cycle/nm can be taken as 0, although the values above a frequency of 0.01 cycle/nm are almost negligible. We emphasize this because in the figures of Buchsbaum and Gottschalk[2] this Fourier transform clearly vanishes at frequencies even lower than 0.01 cycle/nm, which is not in accord with our results. The resolution in their study is 12.5 times lower than that in the present calculation. This difference in resolution is expressed, for example, in the fact that Buchsbaum and Gottschalk had values at only 3 frequency points inside the interval of 0–0.01 cycle/nm, whereas this study has 40 points and hence is much more accurate.

The transform for the $\bar{x}_\lambda$ function also nearly disappears at frequencies greater than 0.02 cycle/nm, and, as we have already mentioned, the behavior of the Fourier transform for $\bar{z}_\lambda$ is similar to that for $\bar{y}_\lambda$, except that the latter varies more slowly with the frequency. This leads us to believe that what holds good for $\bar{y}_\lambda$ at 0.01 and 0.02 cycle/nm should apply to $\bar{z}_\lambda$ at frequencies of 0.02 and 0.04 cycle/nm. In this case the transform nearly vanishes at a frequency of 0.04 cycle/nm or above.

## MATHEMATICAL RECONSTRUCTION OF THE COLOR-MATCHING FUNCTIONS

On the basis of the results described above we have tried to reconstruct mathematically the color-matching functions with the use of formula (1) for two limiting frequencies: 0.02 and 0.05 cycle/nm. Within the limitations considered above with respect to the application of the sampling theorem, the expressions that we will use for the mathematical reconstruction of the distinct color-matching functions will be, in the case of $f_1 = 0.02$ cycle/nm,

$$M'(\lambda) = \sum_{n=15}^{30} M\left(\frac{n}{2f_1}\right)\mathrm{sinc}\left[2f_1\left(\lambda - \frac{n}{2f_1}\right)\right] \qquad (2)$$

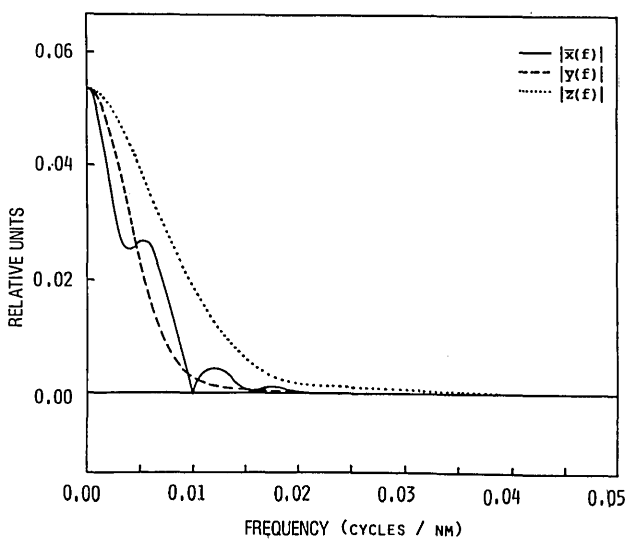


Fig. 1. FFT modulus for different CIE 1931 standard-observer color-matching functions. Ordinates are in arbitrary units.

**Table 1. Original $\bar{x}_\lambda$ and Its Reconstruction Sampled at Two Intervals**

| $\lambda$ (nm) | $\bar{x}_\lambda$(original) | $\bar{x}_\lambda(\Delta\lambda = 10$ nm) | $\bar{x}_\lambda(\Delta\lambda = 25$ nm) |
|---|---|---|---|
| 375 | 0.0007416 | 0.0006141 | 0.0007416 |
| 395 | 0.0076500 | 0.0076036 | 0.0010724 |
| 415 | 0.0776300 | 0.0771594 | 0.1135753 |
| 435 | 0.3285000 | 0.3317251 | 0.3036837 |
| 455 | 0.3187000 | 0.3200262 | 0.3145065 |
| 475 | 0.1421000 | 0.1428042 | 0.1421000 |
| 495 | 0.0147000 | 0.0151026 | 0.0144864 |
| 515 | 0.0291000 | 0.0295138 | 0.0368710 |
| 535 | 0.2257499 | 0.2264903 | 0.2193717 |
| 555 | 0.5120501 | 0.5128741 | 0.5131871 |
| 575 | 0.8425000 | 0.8434121 | 0.8425000 |
| 595 | 1.0567000 | 1.0562970 | 1.0567290 |
| 615 | 0.9384000 | 0.9401727 | 0.9322011 |
| 635 | 0.5419000 | 0.5408514 | 0.5464982 |
| 655 | 0.2187000 | 0.2179515 | 0.2181796 |
| 675 | 0.0636000 | 0.0631961 | 0.0636000 |
| 695 | 0.0158400 | 0.0151778 | 0.0153738 |
| 715 | 0.0041094 | 0.0036076 | 0.0050038 |
| 735 | 0.0009999 | 0.0006371 | 0.0001718 |
| 755 | 0.0002348 | −0.0000461 | 0.0006974 |

**Table 2. Original $\bar{y}_\lambda$ and Its Reconstruction Sampled at Two Intervals**

| $\lambda$ (nm) | $\bar{y}_\lambda$(original) | $\bar{y}_\lambda(\Delta\lambda = 10$ nm) | $\bar{y}_\lambda(\Delta\lambda = 25$ nm) |
|---|---|---|---|
| 375 | 0.0000220 | 0.0002418 | 0.0000220 |
| 395 | 0.0002170 | 0.0004677 | −0.0025288 |
| 415 | 0.0021800 | 0.0024596 | 0.0079333 |
| 435 | 0.0168400 | 0.0173670 | 0.0095020 |
| 455 | 0.0480000 | 0.0485477 | 0.0532351 |
| 475 | 0.1126000 | 0.1131859 | 0.1126000 |
| 495 | 0.2586000 | 0.2582759 | 0.2517048 |
| 515 | 0.6082000 | 0.6093491 | 0.6069945 |
| 535 | 0.9148501 | 0.9146398 | 0.9230018 |
| 555 | 1.0000000 | 0.9999541 | 0.9948903 |
| 575 | 0.9154000 | 0.9155146 | 0.9154000 |
| 595 | 0.6949000 | 0.6948101 | 0.6992706 |
| 615 | 0.4412000 | 0.4415356 | 0.4333621 |
| 635 | 0.2170000 | 0.2162775 | 0.2238835 |
| 655 | 0.0816000 | 0.0810757 | 0.0785629 |
| 675 | 0.0232000 | 0.0228501 | 0.0232000 |
| 695 | 0.0057230 | 0.0053077 | 0.0078686 |
| 715 | 0.0014840 | 0.0011474 | −0.0015158 |
| 735 | 0.0003611 | 0.0000903 | 0.0030629 |
| 755 | 0.0000848 | −0.0001439 | −0.0014408 |

and, for $f_1 = 0.05$ cycle/nm,

$$M'(\lambda) = \sum_{n=36}^{75} M\left(\frac{n}{2f_1}\right)\mathrm{sinc}\left[2f_1\left(\lambda - \frac{n}{2f_1}\right)\right], \qquad (3)$$

where we have substituted the interval of the sum in formula (1) for that in which the function has values $M(\lambda)$ significantly different from 0 and that will give us an approximate analytical reconstruction $M'(\lambda)$ of the corresponding color-matching function.

As can be observed, when $f_1 = 0.02$ cycle/nm, 16 terms appear in the sum of the formula, and thus we sample values of the corresponding function, at intervals of 25 nm, from 375 to 750 nm. When $f_1 = 0.05$ cycle/nm, the result is 40 terms in the sum of the formula with values for the function at intervals of 10 nm, from 360 to 750 nm. The results are shown in Tables 1–3, in which the values for the functions and for the two reconstructions for 20 wavelengths in the visible spectrum are listed.

If we analyze the data in Tables 1–3 we find, as might be expected, that the three functions reconstructed at intervals of 10 nm are similar to the original ones, their values being identical to the second decimal place, and generally to the third, even without rounding off. It can be seen that the greatest similarities occur with the corresponding function at its highest values and thus the relative error at these wavelengths is small.

The results for the functions reconstructed at $f_1 = 0.02$ cycle/nm are also satisfactory for the $\bar{x}_\lambda$ and $\bar{y}_\lambda$ functions but not so good for $\bar{z}_\lambda$, as we had predicted. In Fig. 2 the original $\bar{x}_\lambda$ function is shown superimposed on the one reconstructed at intervals of 25 nm. The slight differences shown in Table 1, which also include the inherent error involved in computer calculations, are appreciable only in tiny variations in the first peak of the function. When the same thing is done for the $\bar{y}_\lambda$ function, no differ-

**Table 3. Original $\bar{z}_\lambda$ and Its Reconstruction Sampled at Two Intervals**

| $\lambda$ (nm) | $\bar{z}_\lambda$(original) | $\bar{z}_\lambda(\Delta\lambda = 10$ nm) | $\bar{z}_\lambda(\Delta\lambda = 25$ nm) |
|---|---|---|---|
| 375 | 0.0034860 | 0.0021525 | 0.0034860 |
| 395 | 0.0362100 | 0.0351699 | 0.0023658 |
| 415 | 0.3713000 | 0.3680698 | 0.5474699 |
| 435 | 1.6229600 | 1.6372050 | 1.4964980 |
| 455 | 1.7441000 | 1.7499310 | 1.7201910 |
| 475 | 1.0419000 | 1.0436760 | 1.0419000 |
| 495 | 0.3533000 | 0.3532304 | 0.3718955 |
| 515 | 0.1117000 | 0.1133354 | 0.1049390 |
| 535 | 0.0298400 | 0.0311522 | 0.0301580 |
| 555 | 0.0057499 | 0.0066123 | 0.0053330 |
| 575 | 0.0018000 | 0.0024769 | 0.0018000 |
| 595 | 0.0010000 | 0.0014678 | 0.0011592 |
| 615 | 0.0002400 | 0.0006775 | 0.0000930 |
| 635 | 0.0000300 | 0.0004128 | 0.0001911 |
| 655 | 0 | 0.0003520 | −0.0001002 |
| 675 | 0 | 0.0003265 | 0 |
| 695 | 0 | 0.0003033 | 0.0001006 |
| 715 | 0 | 0.0002828 | −0.0001667 |
| 735 | 0 | 0.0002649 | 0.0001695 |
| 755 | 0 | 0.0002491 | −0.0001068 |

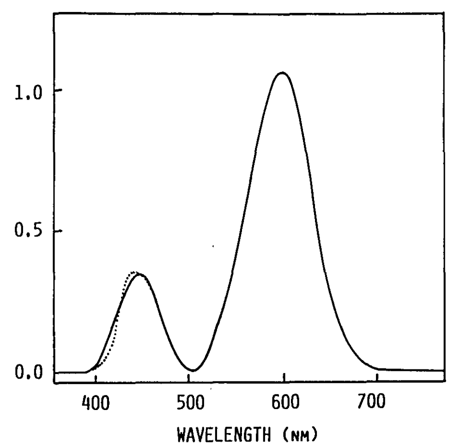


Fig. 2. Original $\bar{x}_\lambda$ (dotted curve) and its reconstruction sampled at intervals of 25 nm (solid curve).

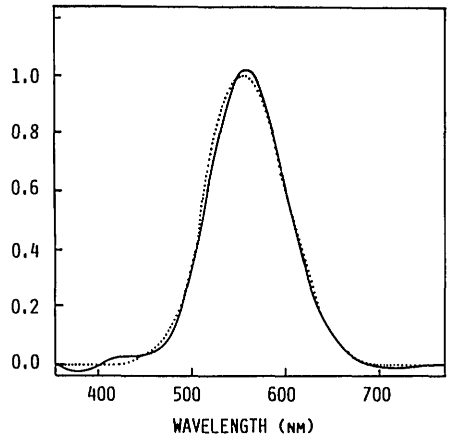


Fig. 3. Original $\bar{y}_\lambda$ (dotted curve) and its reconstruction sampled at intervals of 50 nm (solid curve).

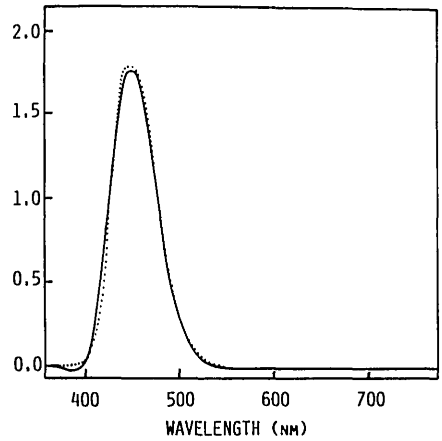


Fig. 4. Original $\bar{z}_\lambda$ (dotted curve) and its reconstruction sampled at intervals of 25 nm (solid curve).

ence whatsoever is to be observed, and, for this reason, we have not included the corresponding figure.

Nevertheless, we considered it worthwhile to include a representation of the original $\bar{y}_\lambda$ function together with its reconstruction at $f_1 = 0.01$ cycle/nm, that is, with eight terms in the sum of formula (1), $n$ from 8 to 15, sampled at intervals of 50 nm from 400 to 750 nm (Fig. 3). In this case the reconstructed function is slightly displaced toward the long wavelengths. We have included this figure to show that, although the fitting of the two functions is not excellent, it is no worse than that found by comparing the color-matching functions measured by different normal observers (see Ref. 9, pp. 343–347, 383, and 396). The same can be said for the representation in Fig. 4 of the reconstruction of the $\bar{z}_\lambda$ function at intervals of 25 nm.

We made a numerical estimation of the differences between the original and the reconstructed functions (Table 4) by calculating the mean absolute error, defined as

$$\langle d\rangle = \frac{1}{N}\sum_{\text{vis}}|M(\lambda) - M'(\lambda)|, \tag{4}$$

where $M(\lambda)$ and $M'(\lambda)$ are the original function and the reconstructed one, respectively; $N = 400$ if it is implied that we have sampled values of the functions at intervals of 1 nm, from 360 to 759 nm.

The results in Table 4 support the conclusions to be drawn from the analysis of Fig. 1 as to the number of decimal places to which the reconstructed function coincides with the original. Of $\bar{x}_\lambda$, $\bar{y}_\lambda$, and $\bar{z}_\lambda$, the set of functions that fits most reliably is $\bar{x}_\lambda$, although $\bar{y}_\lambda$ is equally reliable at $\Delta\lambda = 25$ nm.

Furthermore, if we calculate a relative error for the reconstruction, dividing the values of $\langle d\rangle$ in Table 4 by the mean value of the respective function, i.e.,

$$\langle r\rangle = \langle d\rangle \Big/ \frac{1}{N}\sum_{\text{vis}} M(\lambda), \tag{5}$$

we obtain the values of $\langle r\rangle$ indicated in Table 4, which may be understood as a percentage of error in the reconstruction. Thus the reconstructions imply errors of less than 1% and 2% when $\Delta\lambda = 10$ nm and $\Delta\lambda = 25$ nm, respectively, with the exception that, for $\bar{z}(\lambda)$, the error is 7% when $\Delta\lambda = 25$ nm.

We can conclude that the reconstructions of the color-matching functions are always satisfactory when the color-matching functions are sampled at intervals of 10 nm, which means that it is possible to reduce the number of the experimental measurements necessary for their determination. Intervals of 25 nm, involving measurements at 16 or 17 wavelengths, may even give acceptable results. Nonetheless, the calculation of the color-matching functions is carried out experimentally on functions that refer to real primary colors, with all three functions being measured simultaneously, and, for this reason, the frequency of sampling depends on the results obtained for $\bar{z}_\lambda$, the function that behaves least reliably. Whatever the case, the frequency of sampling will always depend on the experimental objectives laid down.

The $\bar{y}_\lambda$ function is of great interest because it coincides with the photopic luminous efficiency function $V_\lambda$, which results from independent experimental measurement. This function is of summary importance in photometry, and so a reduction in the number of spectral measurements necessary for its determination would be extremely useful; in fact in our analysis we get the best results for this function. We also have at our disposal a mathematical expression with a number of terms in the sum that can be altered according to the degree of reliability desired.

We also conclude that our method for reproducing color-matching functions is applicable to obtaining values for a determined function at wavelengths for which it has not been measured, for example, if the measurements have been made at 5 nm, and values at 1 nm are required. It is plausible that this mathematical analysis may also be used in other spectral functions in color vision as it is reasonable to presume that the application of Fourier transforms

**Table 4. Mean Absolute Error $\langle d\rangle$ and Relative Error $\langle r\rangle$ for Two Reconstructions of the Color-Matching Functions Analyzed[a]**

| | $\Delta\lambda = 10$ nm | | $\Delta\lambda = 25$ nm | |
|---|---|---|---|---|
| Function | $\langle d\rangle$ | $\langle r\rangle$ | $\langle d\rangle$ | $\langle r\rangle$ |
| $\bar{x}_\lambda$ | 0.000687 | 0.002573 | 0.004527 | 0.016955 |
| $\bar{y}_\lambda$ | 0.001625 | 0.006086 | 0.005323 | 0.019936 |
| $\bar{z}_\lambda$ | 0.001716 | 0.006426 | 0.017966 | 0.067288 |

[a] $\Delta\lambda$, interval of sampling.

to some of them will produce analogous results, as Barlow[4] has shown with the Smith–Pokorny fundamentals. In accord with Barlow's results, we have also found that chromatic information above a frequency around 0.02 cycle/nm, must be poor at stimulating the color vision system.

## REFERENCES

1. W. S. Stiles, G. Wyszecki, and N. Ohta, "Counting metameric object-color stimuli using frequency-limited spectral reflectance functions," J. Opt. Soc. Am. **67,** 779–784 (1977).
2. G. Buchsbaum and A. Gottschalk, "Chromaticity coordinates of frequency-limited functions," J. Opt. Soc. Am. A **1,** 885–887 (1984).
3. L. T. Maloney, "Evaluation of linear models of surface spectral reflectance with small numbers of parameters," J. Opt. Soc. Am. A **3,** 1673–1683 (1986).
4. H. B. Barlow, "What causes trichromacy? A theoretical analysis using comb-filtered spectra," Vision Res. **22,** 635–643 (1982).
5. T. Benzschawel, M. H. Brill, and T. E. Cohn, "Analysis of human mechanisms using sinusoidal spectral power distributions," J. Opt. Soc. Am. A **3,** 1713–1725 (1986).
6. J. W. Goodman, *Introduction a l'Optique de Fourier et a l'Holographie* (Masson, Paris, 1972), pp. 20–24.
7. E. I. Stearns, "The determination of weights for use in calculating tristimulus values," Color Res. Appl. **6,** 210–212 (1981).
8. W. Erb and M. Krystek, "Truncation error in colorimetric computations," Color Res. Appl. **8,** 17–22 (1983).
9. G. Wyszecki and W. S. Stiles, *Color Science* (Wiley, New York, 1982).